# The ion velocity (Bohm–Chodura) boundary condition at the entrance to the magnetic presheath in the presence of diamagnetic and E×B drifts in the scrape-off layer

P. C. Stangeby
*University of Toronto Institute for Aerospace Studies, Ontario, M3H 5T6, Canada, and JET Joint Undertaking, Abingdon, Oxon, OX14 3EA, United Kingdom*

A. V. Chankin[a)]
*JET Joint Undertaking, Abingdon, Oxon, OX14 3EA, United Kingdom*

(Received 9 September 1994; accepted 23 November 1994)

In the absence of drifts, the Bohm–Chodura criterion gives that the fluid velocity parallel to the magnetic field reaches the ion acoustic speed at the entrance to the magnetic presheath. The changes to this criterion are derived for the situation where poloidal $E\times B$ drifts are present. (It was shown earlier that diamagnetic drifts do not influence this criterion.) Here $E\times B$ drifts can cause the parallel fluid velocity at the magnetic presheath entrance to become supersonic, subsonic, or reversed (negative). © *1995 American Institute of Physics.*

## I. INTRODUCTION

Plasma particles are deposited in the scrape-off layer, SOL, of magnetically confined plasmas, either directly by the ionization of neutrals, or by cross-field transport from the ionization region. In the simplest picture these particles are removed by transport along the magnetic field in the SOL to the particle sink constituted by the solid surface of a limiter or divertor plate. Such flow, at the most basic level, results from the pressure gradient that arises along the SOL (along **B**) due to the fact that the solid surface is a sink for charged particles, which depresses the local pressure. Other parallel-to-**B** forces may also be allowed for, including coupling to impurities, viscosity, etc.

A quite separate type of sink action in the SOL should also be considered: that due to diamagnetic and **E×B** drifts. Consider the example of a divertor configuration and its projection in the poloidal plane, Fig. 1. In this projection the component of the parallel flow velocity, $v_\parallel$, can be quite small: $\sin\theta v_\parallel$, where $\sin\theta \equiv B_\theta/B$, $B_\theta$=the poloidal magnetic field, and $B$=the total magnetic field. Generally, there is a radial (cross-field) electric field in the SOL, $E_x$; see Fig. 2. There are a number of factors contributing to the existence of this electric field, but the simplest cause of its existence is the following: (a) A radial electron temperature gradient generally exists; (b) the limiter/divertor target is usually electrically conducting and thus constitutes an equipotential surface (we will define $V=0$ there); and (c) each plasma/magnetic flux tube in the SOL is separated, at its ends, from the solid surface by an electrostatic sheath, the potential drop across which is $\sim 3kT_e/e$ (at least, for locally ambipolar outflow); that is, the plasma is at a higher potential than the solid surface. Since $T_e(x)$ generally falls with $x$, then so does the electrostatic potential of the plasma, and so $E_x$ points radially outward (for the simplest case):

$$E_x = |\psi_w| \frac{kT_e}{e\lambda_{T_e}}, \tag{1}$$

where $|\psi_w|$ is the potential drop across the electrostatic sheath normalized by the electron temperature, $\sim 3$ for ambipolar outflow of a hydrogenic plasma, and here we have assumed that $T_e(x) \propto \exp(-x/\lambda_{T_e})$, with $\lambda_{T_e} > 0$. This electric field is orthogonal to **B** and results in an **E×B** drift of the plasma in the third orthogonal direction, giving a drift velocity component in the poloidal plane of $v_{E\times B} \approx E_x/B$. This velocity can be comparable to the projected parallel velocity; consider the example $|\psi_w|=3$, $\lambda_{T_e} = 10^{-2}$ m, $T_e=30$ eV, $v_\parallel \approx c_s$, the acoustic speed, $c_s \equiv [k(T_e+T_i)/m]^{1/2}$, say $5\times10^4$ m/s, $B=3$ T, $B_\theta/B=0.1$, and $v_\parallel \sin\theta = 5\times10^3$ m/s, while $v_{E\times B} = 3\times10^3$ m/s. Clearly, it would not be correct in such a situation to neglect this contribution to the SOL sink action.

There are also the diamagnetic electron and ion drifts to be considered. Generally radial plasma pressure gradients exist, $\partial p_e/\partial x$, $\partial p_i/\partial x$—contributed to by both the (generally) decaying density and temperature profiles, and this results in an ion drift in the poloidal plane of $\pm(en|B_\phi|)^{-1}\,\partial p/\partial x$. This is readily shown to also be potentially significant compared with $v_\parallel \sin\theta$.

Accordingly, in recent years a number of models and codes used for SOL analysis have incorporated these drift terms[1–8] (and also the closely related drifts in the other cross-field direction), and in some cases large differences have been found, compared with the neglect of these terms. In such an analysis, the question of *boundary conditions* has to be addressed.

In the absence of drifts, and assuming the solid surface is perpendicular to the $v_\parallel$ direction, then the Bohm criterion[9] applies, giving that $v_{\parallel_{SE}} \geq c_s$, where SE≡sheath edge, i.e., where the plasma flux tube interfaces with the Debye sheath. Generally, the solid surface is not orthogonal to the $v_\parallel$ direction, and in that case—again ignoring drifts—one has the Chodura[10,11] criterion, which also gives that $v_\parallel \geq c_s$ at the end of the plasma flux tube, although now the location of the latter is not the (Debye) sheath edge, but the magnetic

[a)]Permanent address: INF Russian Scientific Centre "Kurchatov Institute," Institute for Nuclear Fusion, Moscow, Russia.

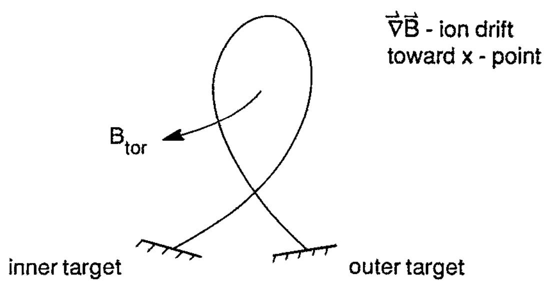


FIG. 1. A poloidal divertor shown in the poloidal cross section.

presheath edge, MPSE, which is located slightly farther from the surface (see later discussions).

What should be done about the velocity boundary condition when drifts are present? The intuitive and sometimes-used procedure is to assume that at the end of the plasma flux tube, MPSE, the total poloidal velocity should satisfy the Bohm–Chodura (BC) criterion, which in the marginal (i.e., equality) form is (for $|B_{tor}|\approx|B|$)

$$\sin\theta\, v_{\|}+\frac{E_x}{B}-\frac{e}{enB}\frac{\partial p_i}{\partial x}=\sin\theta\, c_s. \tag{2}$$

There is not actually any justification for this assumption, and the matter requires more detailed consideration. With regard to the contribution of the diamagnetic drift, this has been carried out,[12] and it was concluded that this drift does not contribute to the boundary condition, i.e., does *not* give flow to the surface. We do not consider this drift further here, and focus on the contribution of $v_{E\times B}$ to the velocity boundary condition. To state the final conclusion of the present study: this drift is found to contribute to the boundary condition; further, the intuitive prescription, Eq. (2) (without the diamagnetic term), is found to be a first approximation to the general result.

The paper is divided as follows. In Sec. II the Bohm–Chodura criterion is briefly reviewed. In Sec. III the particle balance in the MPS is considered, allowing for drift effects. This shows the necessity of establishing an expression for the electric fields in the MPS, both perpendicular to the surface, $E_y$, and along it, $E_x$. Before doing this, in Sec. IV, a simple illustration is given of the approach being taken in the present paper, to act as a "road map" for the full analysis of Secs. V–IX. In Sec. V, expressions are found for the two fields, under certain simplifying assumptions. In Sec. VI the particle balance equation is returned to and evaluated using the approximations for $E_x$ and $E_y$. In Sec. VII the momentum balance in the MPS is considered. In Sec. VIII the results of the particle equation of Sec. VI and the momentum equation of Sec. VII are combined to give the equivalent to the BC criterion, allowing for drifts, which is the principal result of the paper. In Sec. IX this new boundary condition is expressed in a more transparent form. In Sec. X an indication is given on how this boundary condition could actually be used in models and codes.

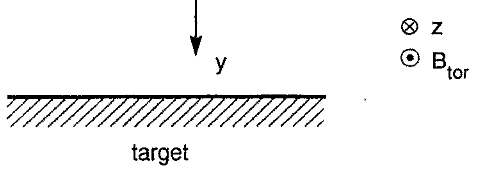


FIG. 2. The poloidal plane at the target.

## II. THE BOHM–CHODURA, BC, CRITERIA

We consider first the case of no drifts.

At the entrance to the Debye sheath, the ion drift velocity into the sheath must be at least equal to the acoustic speed, Bohm criterion.[9] If this is not the case, then the rate of decrease of $n_i$ (with respect either to the spatial variable $s$ measured in the flow direction, with $s=0$ at the sheath entrance where $n_e=n_i=n_0$—or with respect to potential $\phi$, where $\phi=0$ at $s=0$ and $\phi$ necessarily decreases going into the Debye sheath, since that is a region of net positive space charge density) will be greater than the rate of change of $n_e$ with respect to $s$ or $\phi$. That will result in the contradiction of a Debye sheath with net negative charge density. This is readily demonstrated by assuming for the electron density the Boltzmann relation:

$$n_e=n_0\exp(e\phi/kT_e), \tag{3}$$

while for the ions one has the conservation of particles and momentum:

$$\frac{d}{ds}(n_i v)=0, \tag{4}$$

$$m_i n_i v\frac{dv}{ds}=-\frac{dp_i}{ds}+eEn_i, \tag{5}$$

where we assume no volume sources, or sinks, no friction, no change of cross-sectional area of the flux tube, etc. From (3) we find from $E=-d\phi/ds$, and assuming the Bohm criterion in the marginal form—where $n_e$ and $n_i$ decrease exactly together, to give quasineutrality, as the flow enters the Debye sheath—that

$$(v_0^2-c_s^2)\left.\frac{dn}{ds}\right|_{s=0}=0, \tag{6}$$

where $v(0)\equiv v_0$ and $c_s\equiv[k(T_e+T_i)/m_i]^{1/2}$ is the acoustic speed. Clearly, the only value of $v_0$ that will permit the plasma density to decrease entering the sheath is $v_0=c_s$, the Bohm criterion. [One may note that Eq. (6), with $v_0$ replaced by $v$, would also hold for a flow with $E=0$. Then, however, $n$ is constant and so the equation is satisfied without requiring $v=c_s$. It is only when the presence of an electric field is required, as in the sheath, and thus $n$ cannot be constant, Eq. (3), that Eq. (6) requires $v=c_s$.]

When $\mathbf{B}$ is at an angle $\theta<90°$ to the solid surface, Chodura[10] (also see Riemann[11]), has shown that, in addition to the Debye sheath with its strong electric field, there arises a magnetic presheath, MPS, where a significant electric field also exists, perpendicular to the surface. This field is needed in order to accelerate the ions in the MPS to reach the acoustic speed perpendicular to the surface at the Debye sheath edge. The scale size of the Debye sheath is the Debye length; the scale size of the magnetic sheath is the ion Larmor radius. The total potential drop across the two sheaths is about $3kT_e/e$, the same as for the normal incidence sheath (where all this drop occurs in the Debye sheath).

The Chodura criterion gives that the drift velocity of the ions along **B** as the flow enters the magnetic presheath is also $c_s$. The demonstration of this is the same as the above [although now, since the magnetic presheath is quasineutral, with $n_e \approx n_i$ throughout, the requirement is that $n_e$ and $n_i$ decrease together (while for the sheath entrance, $n_e$ must decay at least as fast as $n_i$)].

## III. THE EFFECT OF DIAMAGNETIC AND E×B DRIFTS: THE INTUITIVE BOUNDARY CONDITION

The intuitive alteration to the criterion for the entrance to the magnetic presheath is

$$v_y = \sin\theta\, v_{\parallel_0} + \frac{\cos\theta\, E_x}{|B|} - \frac{\cos\theta}{en|B|}\frac{\partial p_i}{\partial x} = \sin\theta\, c_s; \qquad (7)$$

see Ref. 12, also Fig. 1 for definitions. Here we assume the $\nabla$ **B**-ion drift is toward the bottom $x$ point, thus $\mathbf{B}_z$, i.e., $\mathbf{B}_{\text{tor}}$, are in the negative $Z$ direction, and we distinguish $|\mathbf{B}|$ from $|\mathbf{B}_{\text{tor}}|$. That is, due to the presence of the drift terms, the drift velocity at the entrance to the magnetic presheath, $v_{\parallel_0}$, may be greater or less than $c_s$.

This boundary condition is not, however, physically justifiable, since it is not derived from the requirement that $n_e$ and $n_i$ decrease at the same rate entering the magnetic presheath. Instead, we proceed as before; first, consider conservation of ions:

$$\nabla \cdot \mathbf{\Gamma} = 0, \qquad (8)$$

where

$$\mathbf{\Gamma} = \mathbf{\Gamma}_{\parallel} + \mathbf{\Gamma}_{\mathbf{E}\times\mathbf{B}} + \mathbf{\Gamma}_{\nabla_{p_i}}. \qquad (9)$$

We can neglect the diamagnetic term, however, since it is almost entirely divergence-free,[12] that is, while the component of $\mathbf{\Gamma}_{\nabla_{p_i}}$ in the $y$ direction does decrease with $s$ or $\phi$, this decrease is just compensated by the increase in the $x$ component of $\mathbf{\Gamma}_{\nabla_{p_i}}$, i.e., along the surface; see Ref. 12 for further details. It can be shown, by contrast, that little of the $y$ component of $\mathbf{\Gamma}_{\mathbf{E}\times\mathbf{B}}$ is deflected into flow along the surface; the decrease in this flow is taken up by $\mathbf{\Gamma}_{\parallel}$, at least near the magnetic presheath entrance; closer to the Debye sheath most of the particle flux is taken up by the strong flux in the $y$ direction given by $\frac{1}{4}r_{\text{L}}^2\nabla^2[(\mathbf{E}\times\mathbf{B})/B^2]$, proportional to $d^2E_y/dy^2$,[13] where $r_{\text{L}}$=ion Larmor radius; we assume $d^2E_y/dy^2|_{s=0}$ to be negligible.

From (8), we have

$$\frac{d}{dy}[n(\cos\theta\, v_D + \sin\theta\, v_{\parallel})] = -\frac{d\Gamma_x}{dx}, \qquad (10)$$

where $v_D \equiv E_x/|B|$ is the drift in the poloidal plane, and orthogonal to **B**.

In order to proceed further, it is clearly necessary to develop expressions for $E_x(y)$, or equivalently $E_x(\phi)$, and also for $\Gamma_x = -\cos\theta n E_y/|B|$, and thus for $E_y(x)$. We defer this, however, to Sec. V.

Before proceeding to the full analysis, in the next section we illustrate the approach that will be taken by a much simplified (indeed overly simplified) example. Unfortunately, when all the necessary terms are included in the analysis, it becomes rather cumbersome, and perhaps opaque. The simplified example of the next section, it is hoped, will constitute a "road map" to the more extended analysis that follows.

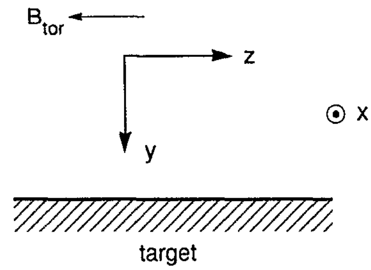


FIG. 3. The toroidal–poloidal plane at the target.

## IV. A SIMPLE ILLUSTRATION OF THE APPROACH TO BE TAKEN

We will start by neglecting the right-hand side, RHS, of Eq. (10), thus the change in parallel flux is taken up by a change in the $v_D$-drift flux.

For a momentum equation we use Eq. (5), with $s \to s_{\parallel}$ and $ds_{\parallel} = dy/\sin\theta$, i.e., drift effects are ignored.

As mentioned at the end of the last section, we need to find $E_x(y)$ or $E_x(\phi)$. We now proceed to do this.

We consider the case where the $\nabla B$ ion drift is toward the X point, Fig. 1, and we focus on the outer target. The Cartesian coordinate system is shown in Fig. 2, in the poloidal plane projection, and Fig. 3, in the toroidal section. Thus $\mathbf{B}_{\text{tor}}$ is in the negative $Z$ direction.

For illustration, consider the simple case where plasma fluxes to each part of the target are ambipolar, and that the total potential drop in the MPS plus sheath is $|\psi_w|kT_e/e$, where $|\psi_w|$ does not vary across the target. Typically, $|\psi_w| \approx 3$ for hydrogenic plasmas.[10] Assume also that $T_e(x) = T_e(o)e^{-x/\lambda_{T_e}}$, then one will have Eq. (1). Thus, an **E×B** drift will arise in the $y$ direction, and

$$v_D(y=0) = |\psi_w|kT_e/e|B|\lambda_{T_e}. \qquad (11)$$

For the system specified here, this drift will be into the target on the SOL plasma side of the separatrix, and out of the target on the private plasma side of the separatrix (where $\lambda_{T_e} < 0$).

In order to find how $v_D$ varies with $y$, consider Fig. 4, where two electrostatic potential curves versus $y$ are shown, one for $x=0$ where $T_e = T_1$, the other for $x = \Delta x$ where

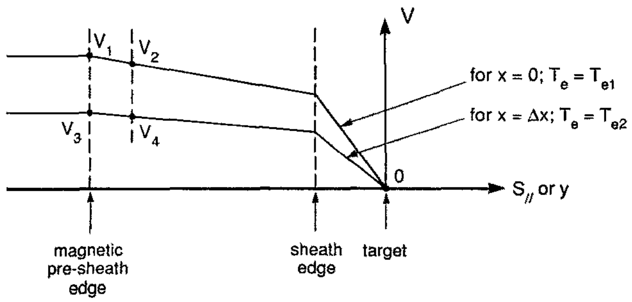


FIG. 4. The poloidal (or along-**B**) variation of the electrostatic potential in the magnetic presheath and sheath at two radial locations, $x=0$, $\Delta x$.

$T_e = T_2$ (although the second profile is shown as being lower than the first; this will not be assumed in the following). We have defined a second potential $V$:

$$\phi \equiv V - |\psi_w| kT_e/e, \tag{12}$$

as this is convenient for the typical case of a continuous, electrically conducting divertor plate that gives the equipotential $V=0$ at the target. For clarity, the MPSE is shown in Fig. 4 as occurring at a finite distance from the solid surface. While the Chodura–Riemann solution for the MPS[10,11] shows that most of the potential drop in the MPS occurs over a finite distance, of order $r_L$, the MPS field actually extends to infinity, where it goes asymptotically to zero (in the absence of ionization, friction, etc.). The simplification that $\phi \to 0$ at some finite distance, say at $r_L$, from the solid surface thus requires further attention, and this is dealt with in the Appendix. Here we proceed on the assumption that $\phi=0$ at the MPSE, where $y=0$ and that, for $x=0$, $\phi=-\Delta\phi(\Delta\phi>0)$, at some distance that is $\Delta y$ closer to the solid surface. Thus $E_y(x=0) = -\partial\phi/\partial y = \Delta\phi/\Delta y$, i.e., is finite.

We assume initially that in the MPS, $E_y$ scales with $T_e$ only, and is not influenced by possible $x$ variations of $\psi_w$: if the plasma flow to the surface is nonambipolar, then $|\psi_w|$ will differ from $\sim 3$ (and may thus have an $x$ dependence), however, the changes of $\psi_w$ are taken up within the sheath, not the MPS, i.e., the MPS potential drop is not changed. The portion of the total $|\psi_w|$ that occurs in the MPS has to do with the strength of the total electric force required to turn the ion flow from being sonic along **B** at the MPSE to being sonic perpendicular to the solid surface at the entrance to the Debye sheath. The total magnitude of $|\psi_w|$ has to do with adjusting the electron flux reaching the surface, so that it equals the ion flux, for ambipolar conditions, or is greater/less for net electron/ion current to the surface. Thus, if the flow is nonambipolar, $|\psi_w|$ will be different from $|\psi_w^f|$, the floating or ambipolar value, but the part of $|\psi_w|$ occurring in the MPS will be unchanged, since that is only dependent on the angle between **B** and the surface.[10] (Of course, if $|\psi_w|$ becomes so small that it is less than that needed in the MPS, then a more complex situation arises; we do not consider such cases here.)

The electric field in the MPS $E_y$ will have a more complex structure than the relatively simple dependence on $x$ through $T_e(x)$ assumed here, when the scale length of $x$ variations of $T_e$ is shorter than an ion Larmor radius, $r_L$: it is readily shown that the net $x$ deflection of an ion trajectory in traversing the MPS is $\simeq r_L$; the scale length of $x$ variations of $E_y$ cannot be smaller than this. We also do not consider such cases here, and treat the MPS as quasi-one-dimensional. Thus,

$$E_y(x=\Delta x) = E_y(x=0)\,\frac{T_{e2}}{T_{e1}} = \frac{\Delta\phi}{\Delta y}\frac{T_{e2}}{T_{e1}}. \tag{13}$$

We also have (in abbreviated symbolic form and absolute signs on $\psi$ understood)

$$V_1 = \psi T_{e1}, \tag{14}$$

$$V_2 = \psi T_{e1} - \Delta\phi, \tag{15}$$

$$V_3 = \psi T_{e2}, \tag{16}$$

$$V_4 = \psi T_{e2} - \Delta y\; E_y(x=\Delta x) = \psi T_{e2} - \Delta\phi\; T_{e2}/T_{e1}. \tag{17}$$

Now

$$E_x(y=0) \equiv -[V_3 - V_1]/\Delta x, \tag{18}$$

$$E_x(y=\Delta y) \equiv -[V_4 - V_2]/\Delta x, \tag{19}$$

which gives

$$E_x(y=\Delta y) = E_x(y=0) + \frac{\phi}{\lambda_{T_e}}. \tag{20}$$

Thus

$$v_D(\phi) = v_D(0) + \frac{\phi}{|B|\lambda_{T_e}}. \tag{21}$$

A term, $dv_D/dy$, arises in expanding Eq. (10), which we can now compute from

$$\frac{dv_D}{dy} = \frac{dv_D}{d\phi}\frac{d\phi}{dy}, \tag{22}$$

with

$$\frac{dv_D}{d\phi} = \frac{1}{|B|\lambda_{T_e}}, \tag{23}$$

and from Eq. (3),

$$\frac{d\phi}{dy} = \frac{kT_e}{en}\frac{dn}{dy}. \tag{24}$$

We can now combine the particle conservation equation (10) (setting RHS=0 here) and the momentum equation (5) to eliminate $dv_\parallel/dy$ and thus, with the aid of Eqs. (22)–(24) obtain

$$\frac{dn}{dy}\left(c_s^2 - v_\parallel^2 - \frac{v_D v_\parallel}{\tan\theta} - \frac{v_D v_\parallel}{|\psi_w|\tan\theta}\right) = 0, \tag{25}$$

where we have also used Eq. (11) to replace $\lambda_{T_e}$.

Consider the MPSE, where Eq. (25) becomes

$$\left(c_s^2 - v_{\parallel_0}^2 - \frac{v_{D_0} v_{\parallel_0}}{\tan\theta} - \frac{v_{D_0} v_{\parallel_0}}{|\psi_w|\tan\theta}\right)\left.\frac{dn}{dy}\right|_0 = 0. \tag{26}$$

Now we apply the same reasoning as was done with Eq. (6): at the MPSE the electric field is nonzero and so, following Eq. (3), $dn/dy$ must be nonzero. Thus, we have the modified Bohm–Chodura condition on the parallel flow velocity at the MPSE, $v_{\parallel_0}$, in terms of $c_s$ and the drift velocity $v_{D_0}$. Neglecting the fourth term in the brackets as small compared to the third term gives

$$M_{\text{MPSE}} = -\gamma + \sqrt{\gamma^2+1}, \tag{27}$$

where

$$M \equiv v_{\parallel}/c_s \tag{28}$$

and

$$\gamma \equiv v_{D_0}/(2c_s \tan\theta). \tag{29}$$

It may be noted that this result differs from the simple intuitive result of Eq. (7) namely,

$$M_{\text{MPSE}}^{\text{intuitive}} = 1 - 2\gamma \tag{30}$$

(neglecting diamagnetic drifts). Since we have made a number of unjustifiable assumptions in order to achieve this simple illustration of the approach, it would not be correct to make anything of the difference between Eqs. (27) and (30).

In order to proceed with the full analysis, we now consider the factors that were left out in the foregoing treatment. These are the following.

(1) The RHS of Eq. (10) should not be neglected, that is, gradients in the particle flux along the solid surface effectively constitute particle sinks/sources. This is dealt with in Secs. V and VI.

(2) The momentum equation (5) has similarly neglected particle and momentum sources/sinks associated with the divergence of cross-field flows. This is dealt with in Sec. VII.

(3) We should allow for the fact that nonambipolar flows to the surface may exist and that $\psi_w$ may vary with $x$. This is dealt with in Sec. V.

(4) Rather than assuming that quantities such as $T_e$ have the specific $x$ variation of $\exp(-x/\lambda_{T_e})$, we should allow for arbitrary $x$ variations by assuming

$$T_e(x) = T_e(0)\left(1 + \frac{x}{l_{T_e}}\right), \tag{31}$$

where

$$l_{T_e} \equiv \left(\frac{1}{T_e}\frac{dT_e}{dx}\right)^{-1}, \tag{32}$$

and so $l_{T_e}$ gives the local spatial variation of $T_e$, i.e., $l_{T_e}$ is, in general, a function of $x$ itself.

(5) We have assumed that in the MPS, $E_y$ scales with $T_e$ only. In fact, Chodura's analysis[10] of the MPS gives that near the start of the MPS, the potential varies as

$$\frac{e\phi}{kT_e} = \left(\frac{d_m}{y}\right)^2, \tag{33}$$

where

$$d_m \equiv \sqrt{6}(c_s/\Omega)\cos\theta, \tag{34}$$

and $\Omega$ = ion gyrofrequency.

Thus, $E_y$ has a more complex dependence on $T_e$ than has been assumed, and also a dependence on $T_i$ through $c_s$.

## V. THE ELECTRIC FIELD IN THE MAGNETIC PRESHEATH

As mentioned, we need to know $E_x(y)$ in order to find $v_D(y)$ [needed for the LHS of Eq. (10)] and $E_y(x)$ in order to find $\Gamma_x$ [needed for the RHS of Eq. (10)]. We proceed to find these quantities here, allowing for the refinements indicated in the last section.

The first step is to modify Eq. (13) to allow for the dependence of $\phi$ in the MPS of Eqs. (33) and (34). It is readily seen that in place of Eq. (13) we now have

$$E_y(x=\Delta x) = E_y(x=0)\,\frac{T_{e2}(T_{e2}+T_{i2})}{T_{e1}(T_{e1}+T_{i1})} = \frac{\Delta\phi}{\Delta y}\,\frac{T_{e2}(T_{e2}+T_{i2})}{T_{e1}(T_{e1}+T_{i1})}. \tag{35}$$

For $T_e(x)$ we now assume the form given by Eqs. (31) and (32), and a similar expression for $T_i(x)$. It is also convenient to define, for the sum of $T_e$ and $T_i$,

$$T_e(x) + T_i(x) = [T_e(0) + T_i(0)]\left(1 + \frac{x}{l_{T_{\text{sum}}}}\right), \tag{36}$$

where $l_{T_{\text{sum}}}$ is defined analogously to Eq. (32). We thus have

$$E_y(x=\Delta x) = E_y(x=0)\left(1 + \frac{\Delta x}{l_T}\right), \tag{37}$$

where

$$l_T \equiv [(l_{T_e})^{-1} + (l_{T_{\text{sum}}})^{-1}]^{-1}. \tag{38}$$

This then leads to the simple changes of Eq. (20) and Eq. (21) to

$$E_x(y=\Delta y) = E_x(y=0) - \frac{\phi}{l_T} \tag{39}$$

and

$$v_D(\phi) = v_D(0) - \frac{\phi}{|B| l_T}. \tag{40}$$

(Note the change of sign when using $l_T$ rather than $\lambda_T$.)

Next, we wish to allow for local nonambipolarity. This changes Eqs. (14)–(17) to

$$V_1 = \psi_1 T_{e1}, \tag{41}$$

$$V_2 = \psi_1 T_{e1} - \Delta\phi, \tag{42}$$

$$V_3 = \psi_2 T_{e2}, \tag{43}$$

$$V_4 = \psi_2 T_{e2} - \Delta y E_y(x=\Delta x), \tag{44}$$

where $E_y(x=\Delta x)$ is now given by Eq. (35).

It is readily shown that Eqs. (39) and (40) still hold, but the definitions of $E_x(0)$ and $v_D(0)$ are changed to

$$E_x(0) = -\frac{kT_e}{e}\frac{|\psi_w|}{l_{\text{sh}}}, \tag{45}$$

$$v_D(0)=-\frac{kT_e}{e|B|}\frac{|\psi_w|}{l_{\rm sh}}, \tag{46}$$

where

$$l_{\rm sh}\equiv[(l_{T_e})^{-1}+(l_\psi)^{-1}]^{-1} \tag{47}$$

and

$$l_\psi\equiv\left(\frac{1}{|\psi_w|}\frac{d|\psi_w|}{dx}\right)^{-1} \tag{48}$$

("sh" for sheath). These may be compared with the earlier expressions, Eq. (1) and Eq. (11).

Thus, we have found $E_y(x)$ [Eq. (37)] and $E_x(y)$ [Eq. (39)].

Before leaving this section we now calculate $-d\Gamma_x/dx$, the RHS of Eq. (10):

$$-\frac{d}{dx}\Gamma_x=-\frac{d}{dx}\left(\frac{\cos\theta\, nE_y(x)}{|B|}\right)=\frac{\cos\theta\, nE_y(0)}{|B|l_p}, \tag{49}$$

where we have assumed that

$$n=n_0(1+x/l_n), \tag{50}$$

with $l_n$ defined analogously to Eq. (32). Also,

$$l_p\equiv[(l_T)^{-1}+(l_n)^{-1}]^{-1}. \tag{51}$$

(Note that $l_p$ is close to, but not exactly the same as, the pressure scale length.)

## VI. THE PARTICLE FLUX EQUATION EVALUATED

We are now in a position to evaluate the particle balance equation (10), which gives

$$(\cos\theta\, v_D+\sin\theta\, v_\|)\frac{dn}{dy}+n\cos\theta\frac{dv_D}{dy}+n\sin\theta\frac{dv_\|}{dy}$$
$$=\frac{\cos\theta\, nE_y(o)}{|B|l_p}. \tag{52}$$

First we address the $dv_D/dy$ term in Eq. (52):

$$\frac{dv_D}{dy}=\frac{dv_D}{d\phi}\frac{d\phi}{dy}. \tag{53}$$

From Eq. (40), we have

$$\frac{dv_D}{d\phi}=-\frac{1}{|B|l_T}. \tag{54}$$

Also, from Eq. (3),

$$\frac{d\phi}{dy}=-\frac{kT_e}{ne}\frac{dn}{dy}. \tag{55}$$

Thus, from Eqs. (53)–(55),

$$\frac{dv_D}{dy}=\frac{kT_e}{ne}\frac{dn}{dy}\left(-\frac{1}{|B|l_T}\right). \tag{56}$$

Turning next to the term on the RHS of Eq. (52), since $E_y\equiv-d\phi/dy$, this becomes

$${\rm RHS}=-\frac{\cos\theta\, kT_e}{e|B|l_p}\frac{dn}{dy}. \tag{57}$$

Introducing Eqs. (56) and (57) into Eq. (52), using $v_D\equiv v_D(0)$, and dividing by $\sin\theta$ gives

$$\left(\frac{v_D}{\tan\theta}+v_\|\right)\frac{dn}{dy}-\frac{kT_e}{\tan\theta_e|B|l_T}\frac{dn}{dy}+n\frac{dv_\|}{dy}$$
$$=-\frac{1}{\tan\theta}\frac{kT_e}{e|B|l_p}\frac{dn}{dy}, \tag{58}$$

and so, finally,

$$n\frac{dv_\|}{dy}=-\frac{dn}{dy}\left(\frac{1}{\tan\theta}\frac{kT_e}{e|B|l_p}+\frac{v_D}{\tan\theta}+v_\|-\frac{kT_e}{\tan\theta e|B|l_T}\right). \tag{59}$$

## VII. MOMENTUM BALANCE IN PARALLEL DIRECTION

The momentum equation in the parallel-to-**B** direction is

$$mnv_\|\frac{dv_\|}{ds_\|}=-\frac{dp_i}{ds_\|}+neE_\|+S_m-mv_\|S_p, \tag{60}$$

where $S_p$ and $S_m$ are the particle and momentum "source" rates, respectively, for the parallel direction due to the divergence of cross-field flows. From Eq. (3), and assuming that at the MPS entrance the gradients of electron and ion density are equal, one replaces $neE_\|$ by $-dp_e/ds_\|$. Thus, the first two terms on the RHS of Eq. (60) become

$$-c_s^2 m\frac{dn}{ds_\|}. \tag{61}$$

With regard to the cross-field flow contributions, consider first the contribution from $v_D$, i.e., along the $y$ axis. Defining the coordinate pair $(s_\|,s_\perp)$ in the $(x,y)$ plane, we have

$$dy=\cos\theta\, ds_\perp\quad\text{and}\quad dx=\cos\theta\, ds_\|,\quad\text{etc.} \tag{62}$$

Then

$$S_{py}=-\frac{d}{ds_\perp}\Gamma_\perp=-\frac{d}{ds_\perp}(nv_D) \tag{63}$$

$$=-\cos\theta\frac{d}{dy}(nv_D), \tag{64}$$

while

$$S_{my}=-\frac{d}{ds_\perp}(mv_\|\Gamma_\perp)=-\cos\theta\frac{d}{dy}(mv_\|nv_D). \tag{65}$$

Therefore

$$S_{my}-mv_\|S_{py}=-\cos\theta\, mnv_D\frac{dv_\|}{dy}. \tag{66}$$

With regard to the cross-field contribution from $\Gamma_x$, we have

$$S_{px}=-\frac{d\Gamma_x}{dx}\quad\text{and}\quad S_{mx}=-\frac{d}{dx}(mv_\|\Gamma_x). \tag{67}$$

Thus,

$$S_{mx}-mv_{\|}S_{px}=-m\Gamma_x \frac{dv_{\|}}{dx} \tag{68}$$

$$=\cos\theta\, mn \frac{E_y}{|B|}\frac{dv_{\|}}{dx}. \tag{69}$$

Thus, inserting Eqs. (61), (66), and (69) into Eq. (60), we obtain

$$mnv_{\|}\frac{dv_{\|}}{dy}\sin\theta=-mc_s^2\frac{dn}{dy}\sin\theta-\cos\theta\, mnv_D\frac{dv_{\|}}{dy}$$
$$+\cos\theta\, mn\frac{E_y}{|B|}\frac{dv_{\|}}{dx}, \tag{70}$$

or

$$n\frac{dv_{\|}}{dy}\left(\frac{v_D}{\tan\theta}+v_{\|}\right)=-c_s^2\frac{dn}{dy}+\frac{nE_y}{\tan\theta|B|}\frac{dv_{\|}}{dx}. \tag{71}$$

We rewrite $E_y$ using Eq. (55), thus

$$n\frac{dv_{\|}}{dy}\left(\frac{v_D}{\tan\theta}+v_{\|}\right)=-\frac{dn}{dy}\left(c_s^2+\frac{kT_e}{e|B|\tan\theta}\frac{dv_{\|}}{dx}\right). \tag{72}$$

## VIII. COMBINING THE PARTICLE AND MOMENTUM BALANCE EQUATIONS

We may now eliminate $n(dv_{\|}/dy)$ from Eqs. (59) and (72), while at the same time requiring that $dn/dy\neq 0$, i.e., an electric field is required to exist, since the location is the entrance to the MPS, yet at the same time we have also used in the derivation of these equations that $\delta n_e=\delta n_i$, i.e., the Bohm/Chodura criterion for the entrance to a magnetic presheath. Thus

$$\frac{1}{\tan\theta}\frac{kT_e}{e|B|l_p}\left(\frac{v_D}{\tan\theta}+v_{\|}\right)+\left(\frac{v_D}{\tan\theta}+v_{\|}\right)^2-\left(\frac{kT_e}{\tan\theta\, e|B|l_T}\right)$$
$$\times\left(\frac{v_D}{\tan\theta}+v_{\|}\right)=c_s^2+\frac{kT_e}{e|B|\tan\theta}\frac{dv_{\|}}{dx}. \tag{73}$$

At this point it is worth recalling the overall objective, namely, to find the value of $v_{\|}$ at the entrance to the MPS [where Eq. (73) holds], in terms of the *independent* variables: $\theta$, $T_e$, $T_i$, $|B|$, $l_p$, $l_T$, $l_{\text{sh}}$, $v_D$ (i.e., $E_x$), and $|\psi_w|$. We also note, as an aside, that while $\theta$ and $|B|$ are still independent variables even when the entire SOL plus MPS is considered, the values of the other variables are, in fact, established by solving the SOL particle momentum and energy equations (and allowing for locally nonambipolar flows, i.e., currents), with the appropriate boundary conditions at the MPS entrance, as we are in the process of establishing here.

Note that Eq. (73) also contains $dv_{\|}/dx$. Of course, $dv_{\|}/dx$ is not an independent variable; however, it is convenient to proceed as if it were (see a later discussion), and we define

$$\beta\equiv\frac{kT_e}{e|B|\tan\theta\, c_s^2}\frac{dv_{\|}}{dx}. \tag{74}$$

We also define

$$\frac{dv_{\|}}{dx}\equiv\frac{v_{\|}}{l_v}, \tag{75}$$

where $l_v$ is defined similarly to Eq. (32). Also define

$$\text{Mach number},\quad \mathscr{M}\equiv v_{\|}/c_s, \tag{76}$$

the strength of the drift is given by

$$\gamma\equiv\frac{v_D}{2c_s\tan\theta}. \tag{77}$$

We also define

$$x\equiv 2\gamma+\mathscr{M} \tag{78}$$

and

$$2\alpha\equiv-\frac{kT_e}{\tan\theta\, c_s e|B|l_T}+\frac{kT_e}{c_s e|B|l_p\sin\theta}$$
$$=\frac{kT_e}{\tan\theta\, c_s e|B|l_n}. \tag{79}$$

Inserting Eqs. (74) to (79) into Eq. (73) gives

$$x^2+2\alpha x-\beta-1=0. \tag{80}$$

One therefore solves Eq. (65) to find $x$, i.e., $\mathscr{M}$, i.e., $v_{\|}$ at the entrance to the MPS, in terms of the various variables. The fact that not all these variables are truly independent is not a problem in practice: typically, one will have to solve the SOL equations (with the MPS boundary conditions) *iteratively* to find $l_p$, etc. Thus, one can take the value of $dv_{\|}/dx$ from the previous iteration to use in the next one, until convergence is achieved; see Sec. X.

## IX. THE VELOCITY BOUNDARY CONDITION ALLOWING FOR DRIFTS

To recapitulate: when the particle fluxes into the MPS are locally ambipolar, i.e., no current, then the expression for $v_D$ [i.e., $v_D(0)$] is simple, since $E_x$ is just given by Eq. (18), see Fig. 4, with [Eqs. (14) and (15)]

$$V_1=\frac{kT_{e1}}{e}|\psi_w|\quad\text{and}\quad V_3=\frac{kT_{e2}}{e}|\psi_w|, \tag{81}$$

now [Eq. (32)]

$$T_{e2}\equiv T_{e1}\left(1+\frac{\Delta x}{l_{T_e}}\right). \tag{82}$$

So [see Eq. (1)]

$$E_x=\frac{-kT_e}{e}\frac{|\psi_w|}{l_{T_e}}; \tag{83}$$

thus [see Eq. (11)]

$$v_D=\frac{-kT_e}{e|B|l_{T_e}}|\psi_w|. \tag{84}$$

Note that in the SOL, usually $T_e$ will be decreasing with $x$, i.e., $l_{T_e}<0$, and so $v_D>0$, as noted earlier.

If one wishes to allow for currents flowing in the SOL then $|\psi_w|$ will not be constant with $x$. Then Eqs. (83) and (84) are modified, see Eqs. (45) and (46), with $l_{T_e}$ replaced by

$l_{sh} \equiv (l_{T_e}^{-1} + l_{\psi}^{-1})^{-1}$, Eq. (47). As noted, in practice, one would take the values of $l_{T_e}$, $l_{\psi}$, etc., from the previous iteration to use in the new one. The relation between $|\psi_w|$ and the local current density is

$$j_{\|}=enc_s(1-e^{-|\psi_w^f|-|\psi_w|}), \tag{85}$$

where $\psi_w^f$ is the local ambipolar floating potential; typically $|\psi_w^f|=3$.

We can rewrite $\beta$ as

$$\beta=\frac{-2(x-2\gamma)\gamma l_{sh}}{|\psi_w|l_v}. \tag{86}$$

Also,

$$2\alpha=-\frac{2\gamma l_{sh}}{|\psi_w|l_n}. \tag{87}$$

We can now define

$$a\equiv\frac{1}{|\psi_w|}\frac{l_{sh}}{l_v}, \tag{88}$$

and, using Eqs. (77) and (84),

$$b\equiv-\frac{1}{|\psi_w|}\frac{l_{sh}}{l_n}, \tag{89}$$

and one then finds

$$\frac{v_{\|BMPSE}}{c_s}=-\gamma(2+a+b)+[\gamma^2(a+b)^2+1+4a\gamma^2]^{1/2}. \tag{90}$$

Note: for no drift, $\gamma=0$, then $v_{\|}=c_s$ for all values of $a,b$. Now if $l_{sh}\approx l_v\approx l_n$, $\cos\theta\approx 1$ and if $|\psi_w|\approx 3$ then $a$ and $b$ may be small compared with unity. Then

$$\frac{v_{\|BMPSE}}{c_s}\approx 1-2\gamma. \tag{91}$$

One may note that this, in fact, is the same result, as is given by the intuitive evaluation of the boundary condition at the entrance to the magnetic presheath, Eq. (30) (disallowing diamagnetic drift contributions, as in Ref. 12). In general, however, $a$ and $b$ are nonzero, and may be positive or negative. As an illustration, the values of $v_{\|BMPSE}/c_s$ are given in Fig. 5 for $(a,b)=(0,0)$, $(1,0)$, $(0,1)$, $(1,1)$, $(-1,0)$, $(0,-1)$, and $(-1,-1)$. It is to be noted that $v_{\|BMPSE}$ is generally a function of $x$ through (a) the direct dependence on $c_s$, clear from Eq. (91), but also through $\gamma$, which depends on $c_s$, Eq. (77); the direct dependence of $v_D$, thus $\gamma$, on $T_e(x)$, Eq. (84); the dependencies on $l_{T_e}$, $l_n$, $l_{\psi}$, which will normally vary with $x$. Thus $l_v$, the characteristic length of variation of $v_{\|BMPSE}$, will vary with $x$ (and one needs to establish its value consistently; see Sec. X).

It is evident from Fig. 5 that very large parallel flow velocities, highly supersonic, can result for large values of $|\gamma|$, particularly for large negative values. The implications, more generally, of the new boundary condition, Eq. (90), warrant more detailed consideration, and will be treated separately.

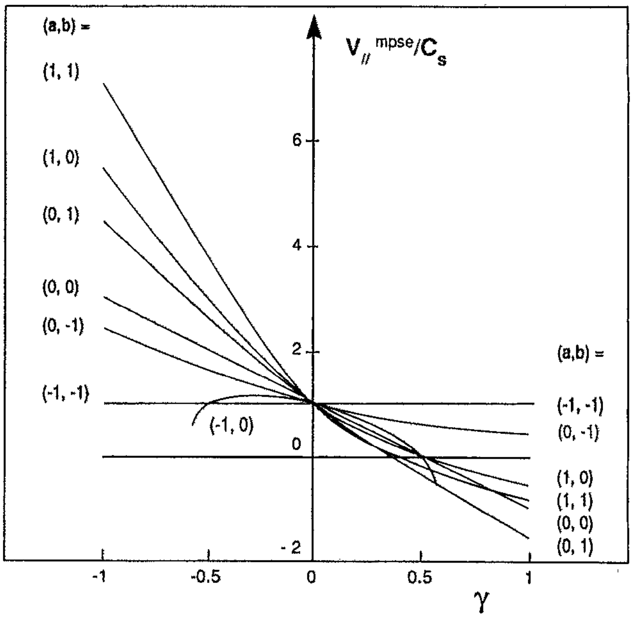


FIG. 5. The parallel-to-**B** drift speed of the plasma at the entrance to the magnetic presheath as a function of the strength of the drift $\gamma=v_{drift}/(2c_s\tan\theta)$, for various values of $a,b$. Here $\theta$ is the angle between **B** and the plane of the target; $a,b$ are ratios of cross-field scale lengths; see the text.

Arguing from experimental evidence on JET, Harbour and Loarte[15] have found that the simple (finite aspect ratio) model of the SOL with the traditional Bohm boundary condition is too restrictive. The experimental results suggest that the Mach number of the plasma flowing toward the limiter on the high-field side could be subsonic. Alternatively, there may be some fundamental problem with the modeling procedure. They suggest that the high value of the local magnetic field or the low value of the glancing angle of incidence may be important.

## X. ITERATING TO FIND $l_v$ AND THE MORE GENERAL QUESTION OF HOW TO USE THE BOUNDARY CONDITIONS

Clearly, $dv_{\|}/dx$ (or $l_v$) is not an independent variable—and one wants to find the value of $l_v$, which is internally consistent. This raises the more general question of how to use the new boundary condition, Eq. (90).

Once drifts are included in a model of the SOL, it is likely that one will be obliged to employ a more-or-less sophisticated computer code, as in Refs. 1–8. Such codes are often time dependent or quasi-time dependent, a feature that lends itself to the incorporation of the boundary condition, Eq. (90). From the previous time step, one will have the two-dimensional (2-D) solution of the SOL equations, and thus will know $n(x)$, $T_e(x)$, $j_{\|}(x)$. Thus one has $l_n$, $l_{T_e}$, $l_p$, $l_T$, $\psi_w(x)$, $l_{\psi}$, and $l_{sh}$—all generally functions of $x$. One also takes $v_{\|BMPSE}(x)$, and thus $l_v(x)$, from the previous iteration, and therefore one can evaluate $a,b,\gamma$ as functions of $x$. From Eq. (90) one thus calculates $v_{\|BMPSE}(x)$ and from that a corrected $l_v$. Reinserting this $l_v(x)$ into the expression for $a$, Eq. (88), one would iterate Eq. (90) to find a consistent $l_v(x)$. One would then proceed to the next time step of the 2-D SOL equations—where one will be able to use a consistent $l_v(x)$ from the previous time step.

## XI. CONCLUSIONS

Poloidal $E \times B$ drifts alter the Bohm–Chodura criterion governing the parallel-to-**B** flow velocity at the entrance to the magnetic presheath, $v_{\|B\mathrm{MPSE}}$. In the absence of drifts $v_{\|B\mathrm{MPSE}} = c_s$, the ion sound speed, while drifts can cause $v_{\|B\mathrm{MPSE}}$ to be supersonic, subsonic, or even reversed (negative).

A new expression for $v_{\|B\mathrm{MPSE}}/c_s$ is obtained, allowing for poloidal $E \times B$ drifts and allowing quantitatively for (a) radial variations of $T_e$, $T_i$, and $n_e$, and (b) radial variations of the floating potential due, for example, to locally nonambipolar flows, i.e., currents.

The derivation is based on the usual assumptions for the magnetic presheath entrance, namely, (i) that $n_e$ and $n_i$ vary together (as a function of distance or electrostatic potential), (ii) these density variations are nonzero.

The result, Eq. (90), has as a first approximation the intuitive result, Eq. (91), based on requiring that the total projected poloidal velocity equal $c_s$.

The full expression, Eq. (90), is not expressed in a closed form, since it contains $l_v \equiv (1/v_{\|B\mathrm{MPSE}}) \times (dv_{\|B\mathrm{MPSE}}/dx)$. It is therefore necessary to use Eq. (90) iteratively, which is done most naturally with an edge 2-D fluid code.

## ACKNOWLEDGMENTS

The authors wish to thank Dr. M. Baelmans and Dr. K.-U. Riemann for helpful discussions.

Support by the Canadian Fusion Fuels Technology Project is acknowledged by P. C. Stangeby.

## APPENDIX: ASSUMPTION THAT THE MAGNETIC PRESHEATH STARTS AT A FINITE DISTANCE FROM THE SOLID SURFACE

We return to the unfinished matter referred to in Sec. IV, namely that we have assumed that $E_y(x=0)$ is finite, or alternatively that $dn/dy$, see Eq. (55), is finite at the MPSE. In the Chodura[10] or Riemann[11] analysis, the MPSE is at $y$=minus infinity, and all derivatives go to zero asymptotically there. Our criterion for $v_{\|B\mathrm{MPSE}}/c_s$ at the MPSE, Eq. (73), would only appear to hold, provided $dn/dy \neq 0$ at the MPSE, since if $dn/dy = 0$, then there would appear to be no constraint on the value of $v_{\|B\mathrm{MPSE}}/c_s$ at the MPSE. The resolution of this matter is beyond the compass of the present paper, and is dealt with separately.[14] As Riemann[11] has pointed out, the problem arises from the neglect of ion inertia in the **E×B** direction. When this is explicitly included in the analysis,[14] it is found that the simple procedure employed here of assuming $dn/dy \neq 0$ at the MPSE gives the same result for $v_{\|B\mathrm{MPSE}}/c_s$ at the MPSE as allowing simultaneously for (a) **E×B** ion inertia and (b) for the removal of the MPSE to $y = -\infty$ (where $dn/dy \rightarrow 0$).

[1] H. Gerhauser and H. A. Claassen, Contrib. Plasma Phys. **30**, 89 (1990).
[2] M. Petravic, G. Kuo-Petravic, and T. Arzt, Contrib. Plasma Phys. **28**, 379 (1988).
[3] H. Gerhauser and H. A. Claassen, J. Nucl. Mat. **176&177**, 721 (1990).
[4] D. A. Knoll and A. K. Prinja, J. Nucl. Mat. **176&177**, 562 (1990).
[5] T. D. Rognlien, J. L. Milovich, M. E. Rensink, and G. D. Porter, J. Nucl. Mat. **196–198** 347 (1992).
[6] E. L. Vold, Contrib. Plasma Phys. **32**, 404 (1992).
[7] E. L. Vold, F. Najmabadi, and R. W. Conn, Phys. Fluids B **3**, 3132 (1991).
[8] M. Baelmans, D. Reiter, H. Kever, P. Borner, M. W. Wuttke, T. Pütz, R. Schneider, G. P. Maddison, B. J. Braams, and R. R. Weynants, J. Nucl. Mat. **196–198**, 466 (1992).
[9] D. Bohm, in *The Characteristics of Electrical Discharges in Magnetic Fields*, edited by A. Guthrie and R. K. Wakerling (McGraw-Hill, New York, 1949), Chap. 3, p. 90.
[10] R. Chodura, Phys. Fluids **25**, 1628 (1982).
[11] K.-U. Riemann, Phys. Plasmas **1**, 552 (1994).
[12] A. V. Chankin and P. C. Stangeby, Plasma Phys. Controlled Fusion **36**, 1485 (1994).
[13] F. F. Chen, *Introduction to Plasma Physics* (Plenum, New York, 1974), p. 38.
[14] P. C. Stangeby, Phys. Plasmas **2**, 702 (1995).
[15] P. J. Harbour and A. Loarte, to appear in Nucl. Fusion.